REPORT DOCUMENTATION PAGE

Form Approved
OMB No. 0704-0188

1. REPORT DATE *(DD-MM-YYYY)*	2. REPORT TYPE	3. DATES COVERED *(From - To)*
07-07-2006	Journal Article	

4. TITLE AND SUBTITLE

Mesoporous Carbons with Self-assembled High-activity Surfaces (PREPRINT)

5a. CONTRACT NUMBER

5b. GRANT NUMBER

5c. PROGRAM ELEMENT NUMBER

6. AUTHOR(S)
Kengqing Jian, Trun C. Truong, & Robert H. Hurt (Brown University); Wesley P. Hoffman (AFRL/PRSM)

5d. PROJECT NUMBER

5e. TASK NUMBER
23060529

5f. WORK UNIT NUMBER

7. PERFORMING ORGANIZATION NAME(S) AND ADDRESS(ES)

Air Force Research Laboratory (AFMC)
AFRL/PRSM
9 Antares Road
Edwards AFB CA 93524-7401

8. PERFORMING ORGANIZATION REPORT NUMBER

AFRL-PR-ED-JA-2006-230

9. SPONSORING / MONITORING AGENCY NAME(S) AND ADDRESS(ES)

Air Force Research Laboratory (AFMC)
AFRL/PRS
5 Pollux Drive
Edwards AFB CA 93524-7048

10. SPONSOR/MONITOR'S ACRONYM(S)

11. SPONSOR/MONITOR'S NUMBER(S)
AFRL-PR-ED-JA-2006-230

12. DISTRIBUTION / AVAILABILITY STATEMENT

Approved for public release; distribution unlimited (AFRL-ERS-PAS-2006-173)

13. SUPPLEMENTARY NOTES
Submitted to the journal Carbon.

14. ABSTRACT

There is great interest in the development of improved mesoporous carbons as sorbents [1-3], catalyst supports [4-6], capacitors [7-9], and electrodes [10-12]. The optimization of mesoporous carbons typically focuses on the control of pore structure, surface area, and the number and type of surface functional groups. A porous carbon property that is often overlooked is the crystal structure of the carbon in the immediate vicinity of the internal surfaces. This interfacial structure provides the carbon "platform" for subsequent surface treatment and can thus determine the number of potential active sites for functionalization and influence the final polarity, surface charge density, and/or chemisorptive activity of the carbon material.

15. SUBJECT TERMS

16. SECURITY CLASSIFICATION OF:			17. LIMITATION OF ABSTRACT	18. NUMBER OF PAGES	19a. NAME OF RESPONSIBLE PERSON
a. REPORT	b. ABSTRACT	c. THIS PAGE			Dr. Wesley P. Hoffman
Unclassified	**Unclassified**	**Unclassified**	A	23	19b. TELEPHONE NUMBER *(include area code)* N/A

Submitted to “Carbon”

Mesoporous carbons with self-assembled high-activity surfaces

(PREPRINT)

Kengqing Jian[†], Trung C.Truong[†], Wesley P. Hoffman[††], Robert H. Hurt[†,*]

[†] Brown University, Division of Engineering, 182 Hope Street, Providence, RI 02912

[††] Air Force Research Laboratory, AFRL/PRSM, 10 E. Saturn Blvd., Edwards, CA 93524

Keywords: Porous carbon, Surface properties, Mesophase, Electron microscopy

*Corresponding author.

Tel.: +1 4018632685; fax: +1 4018639120.

E-mail address: Robert_Hurt@brown.edu (R. Hurt).

1. Introduction

There is great interest in the development of improved mesoporous carbons as sorbents [1-3], catalyst supports [4-6], capacitors [7-9], and electrodes [10-12]. The optimization of mesoporous carbons typically focuses on the control of pore structure, surface area, and the number and type of surface functional groups. A porous carbon property that is often overlooked is the crystal structure of the carbon in the immediate vicinity of the internal surfaces. This interfacial structure provides the carbon "platform" for subsequent surface treatment and can thus determine the number of potential active sites for functionalization and influence the final polarity, surface charge density, and/or chemisorptive activity of the carbon material.

It is now becoming possible to control the spatial arrangement of graphene layers through molecular engineering, especially in near-surface regions, through liquid crystal templating using mesophase pitch or related polyaromatic precursors [13-15 Hurt 2002, Chan 2005, Jian 2003]. Liquid crystal templating techniques have been used to fabricate platelet-symmetry carbon nanofibers [15-17 Jian 2003; Jian carbon 2006; Konno H 2004], and nanotubes [14, 18-19 Chan 2005; Mullen 2005a; Mullen 2005b.], all-edge carbon thin films [20 Jian 2005], and porous carbons [21-25; 21 Kim TW 2003; 22 Nancy JNN2003; 23 Gierszal KP, 2004; 24 Gierszal KP 2005; 25 Yoon SB 2005.]. Previous work has established surface anchoring rules for the discotic mesogens in mesophase pitch, which prefer edge-on anchoring onto most (but not all) substrates [13, 26 Hurt 2002, Jian 2003 LC anchoring]. In confined spaces the discotic molecules form unique supramolecular configurations that are often predictable from liquid crystal theory. Figure 1 shows selected configurations that have been reported from previous studies. The further carbonization process can covalently capture the supramolecular assembly order, leading to carbons with controllable physical shape, graphene layer orientation, and in many cases abundant edge sites concentrated at surfaces.

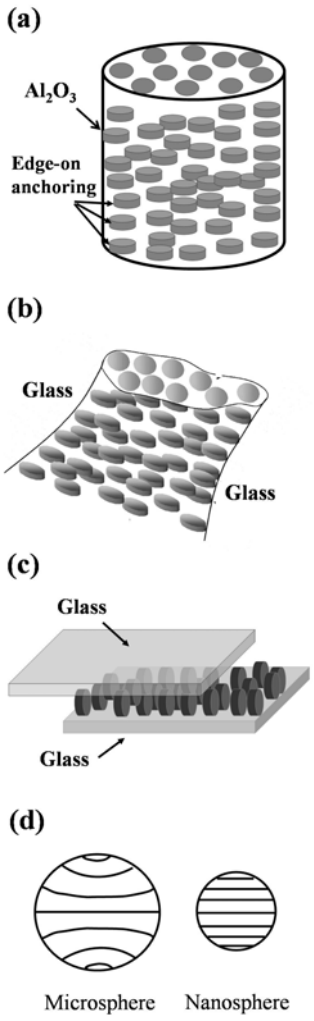

Figure 1. Known discotic molecular configurations caused by micro- and nano-confinement of mesophase pitch in various geometries: (a) cylindrical [15-16 Jian 2003, Jian2006], (b) hour-glass [22 Yang 2003], (c) laminar [21 Jian 2005], and (d) spherical structures, which include Brooks-Taylor mesospheres [27 Brooks and Taylor 1965] observed at micron length scales, and the homogeneous domains favored at the nanoscale [22 Yang et al., 2003]. These structures are selected by the combination of edge-on anchoring (preferred at most interfaces [26 Jian 2003 LC anchoring], and the avoidance of curvature in the director field which produces elastic strain.

Many (but not all) of the new mesophase-derived nanomaterials have surfaces composed solely of graphene edges. Carbon edge sites are generally more active than the atoms in basal planes in a variety of chemical reactions [28-30 Hennig GR, 1966; Thomas JM, 1965; Phillips 1970], and it is reasonable to expect that the edge-rich carbon surfaces would offer advantages for high-density functionalization, heterogeneous electron

transfer, or rapid lithium intercalation and de-intercalation. Recently, it has been reported that graphene edge plane surfaces can have high hydrophilicity [16, 31 Jian Carbon2006; Ye H. 2004], which could be valuable for nanomaterial dispersion and functionalization in biomedical applications. There is need for more work focused on the quantitative characterization of the surface properties of these all-graphene-edge surfaces.

The goal of the current research is to synthesize and characterize a set of new mesoporous carbons in which both the pore structure and the interfacial graphene layer structure have been systematically controlled by liquid crystal templating. We focus on silica templates that cause edge-on discotic anchoring and yield carbons with inner surfaces rich in graphene edge sites. We hypothesize that these all-edge surfaces will have high chemical reactivity, and a second goal of the research is to assess that hypothesis through quantitative measurements of the surface functionalization density following treatment with nitric acid and molecular oxygen. Showing high reactivity on all-edge-site surfaces is key to the applications of a number of new carbon forms whose outer or inner surfaces have high concentrations of exposed edge sites due to perpendicular or tilted graphene layer order.

2. Experimental

2.1 Preparation and structural analysis of mesoporous carbons

The preparation of mesoporous carbons through templating consists of three basic steps: (a) infiltration of porous templates by the carbon precursor, (b) carbonization of the template/precursor composites, and (c) chemical etching of the templates. As a carbon precursor we use HP grade AR-mesophase pitch (Mitsubishi Gas Chemical) made from catalytic polymerization of naphthalene. The templates are controlled pore glass (CPG) from CPG Inc. and silica gel from Aldrich. CPG samples are available in a variety of pore sizes for a range of applications including enzyme immobilization and chromatography. For this study we used CPG templates with mean pore size of about 12 nm, 25 nm, 45 nm, 70 nm, and 100 nm, and silica gel templates with mean pore size of about 6 nm and 15 nm. The CPG templates show uniform and regular pore structures, while silica gels are more irregular. The templates are labeled as CPG-12, CPG-25,

CPG-45, CPG-70, CPG-100, SG-6, and SG-15 with respect to the template type and mean template pore size.

A physical mixture of template powder and lightly ground solid AR-mesophase pitch was heated at 300 ºC for 2 hours in a tube furnace under nitrogen atmosphere, during which the AR precursor exhibits a homogeneous discotic nematic liquid crystalline phase [13, 27 Hurt 2002, Jian 2003], and infiltrates into the template spontaneously by capillary flow. The temperature was then slowly raised to 700 ºC with a heating rate of 4 ºC/min and held for 1 hour to fully carbonize the AR precursor. After cooling to room temperature, the template was removed by hot 3-molar NaOH solution. The resulting carbon product was washed thoroughly with distilled water and oven dried. Some of the carbons were further annealed at temperatures up to 2500 ºC. AR mesophase precursors were also carbonized separately under the same condition without templates. The non-templated carbon was served as the blank reference for the internal porosity test. Thermogravimetric analysis (TGA) was applied to monitor the complete removal of templates. The as-produced porous carbons are labeled as CPG-12-C, CPG-25-C, CPG-45-C, CPG-70-C, CPG-100-C, SG-6-C, and SG-15-C with respect to their template names.

2.2 Surface treatment and characterization of surface activity

To characterize carbon surface activity, selected carbon samples were treated with nitric acid and the total acid site density determined by base titration [32-34 Boehm 1994; Boehm 2002; 32 Pittman 1997]. Two mesoporous carbons (CPG-25-C and CPG-70-C) were treated with 10 wt-% and 70 wt-% HNO_3 solutions for 24 hours at room temperature, then washed thoroughly using distilled/deionized water, and dried in the oven. For the titration, 50 mg of HNO_3-treated carbon powder was added to 20 ml freshly prepared NaOH solution with pH value approximately 11. The pH values of the NaOH/carbon mixture solutions were measured after 18 hours. The pH values of blank NaOH solutions were also measured initially and after 18 hours as a control. The quantities of acidic sites (pKa < 11) were calculated from titrant stoichiometry.

The carbon surface activity can also be characterized for active surface area (ASA) analysis, which is based on the concept of active sites [35-36 Laine NR, 1963; Hoffman 1984], available for oxygen chemisorption [37-38 Hoffman WP , 1991; Hoffman WP, 2000]. Specifically, two mesoporous carbons (CPG-25-C and CPG-100-C) were heated to 950 ºC under vacuum to a pressure below 10^{-6} Pa to clean the surface. The sample was then cooled to a pre-selected adsorption temperature and a known pressure of gas was admitted. For most carbon materials the active surface area is determined by measuring the amount of oxygen chemisorbed at 300 ºC in 24 hours with a starting pressure of 66 Pa. Because chemisorption can be slow, it is more accurate to determine the number of active sites by measuring the amount of gas desorbed. Thus, after evacuation at adsorption temperature, the oxygen complex that forms after adsorption was removed as carbon monoxide and carbon dioxide by heating the sample to 950 ºC in a closed system of known volume. The relative amounts of the two gases formed were measured by trapping out the CO_2 in a liquid nitrogen bath and then measuring the pressure of each gas separately after the completion of desorption. The amounts of CO and CO_2 were then converted to an equivalent oxygen concentration to calculate the ASA covered by the surface complex, based on three assumptions: (1) the chemisorption occurs on the prismatic planes, i.e. the atoms on the edges of the basal planes, which the pioneering work of Hennig [28, 1966] and Thomas [29, 1965] had identified as the sites of attack by molecular oxygen; (2) the complex consists of one oxygen atom per carbon atom; and (3) each carbon atom occupies an area of 0.083 nm^2.

3. Results and discussion

3.1 Morphology, pore structure and crystal structure of mesoporous carbons

Typical morphologies of the mesoporous carbons derived from CPG templates are shown in Figure 2. Although the CPG templates vary widely in pore size (from 12 nm to 100 nm), all the carbons show a similar morphology – they are uniform, bi-continuous solid/gas phases with monodisperse pore size (Figure 2A,B,C) suggesting that the carbons are accurate negative replicas of the original templates (which have a similar appearance). The continuous, interconnected nature of the silica template aids in complete template removal (no template encapsulation) and high-purity carbons. Both

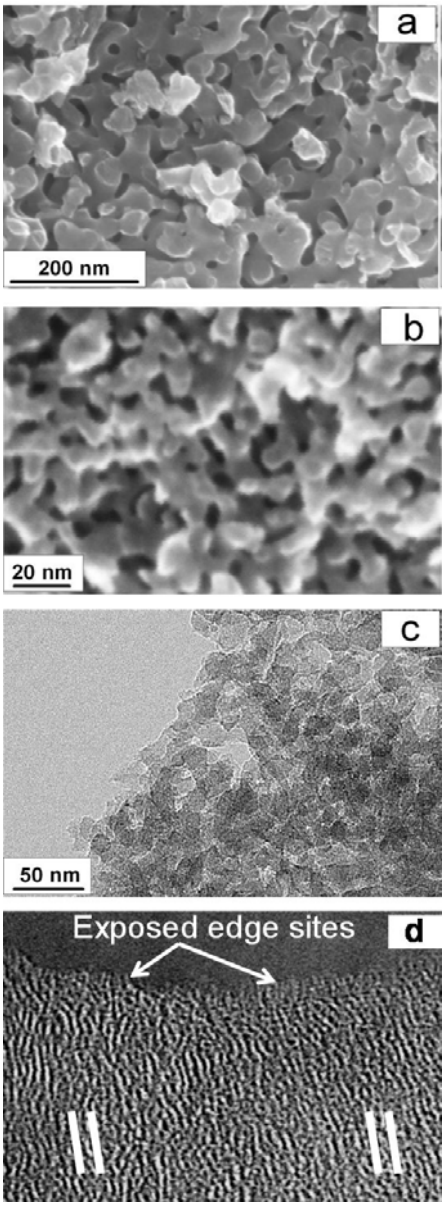

Figure 2. Morphology of CPG template derived mesoporous carbons. (A) SEM image of porous carbon CPG-45-C, which shows the interconnected porous nature of the carbon with solid "grains" of about 40 nm in diameter, (B) SEM image of carbon CPG-12-C, with similar morphology, but on a smaller length scale, (C) TEM image of carbon CPG-12-C, which shows 12 nm interconnected grains, and (D) High-resolution TEM fringe image of the nanophase carbon derived from 100 nm CPG template revealing the graphene layer orientation perpendicular to the mesoporous carbon grain edges, reflecting the original edge-on anchoring state of the liquid crystalline precursor on glass. The white bars in (D) indicate the dominant orientation of the graphene layers. Exposed edge sites can be directly observed on the surface in this particular image.

thermogravimetric and elemental analysis indicate that the carbon is essentially free of residual template. Figure 2D shows that the mesoporous carbons possess an abundance of exposed edge-site-rich surfaces, reflecting the preferred edge-on anchoring state of the discotic AR liquid on glass [13, 26 Hurt 2002, Jian 2003].

Figure 3 shows the morphologies of silica gel templates and the corresponding porous carbons. Silica gel (see Figure 3A) shows a more irregular pore structure (with pore size ranges from several nm to hundreds of nm) compared with CPG templates. The resulting carbons show irregularity (see Figure 3B) due to the negative replica templating of the irregular silica gels. Although silica gel templates exhibit irregular pore structure, they are much less expensive than CPG templates and are thus good alternative candidate templates for achieving practical high-surface-area mesoporous carbons.

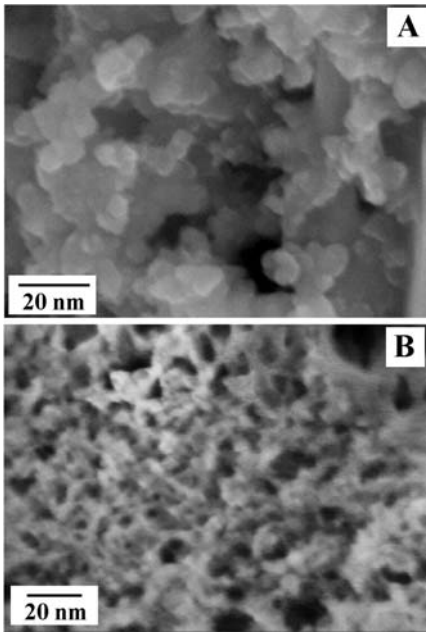

Figure 3. Morphologies of the original silica gel template (A) and resulting mesoporous carbons (B).

Selected porous carbons were post-synthesis annealed at high temperature. Figure 4 shows the XRD patterns of the as-produced 700 ºC porous carbons and the 2500 ºC annealed carbons. Comparing with the broad 002 peak for 700 ºC sample, the sharp 002

peak and its shifting to higher diffraction angles of 2500 ºC annealed sample indicate a much higher degree of crystallinity.

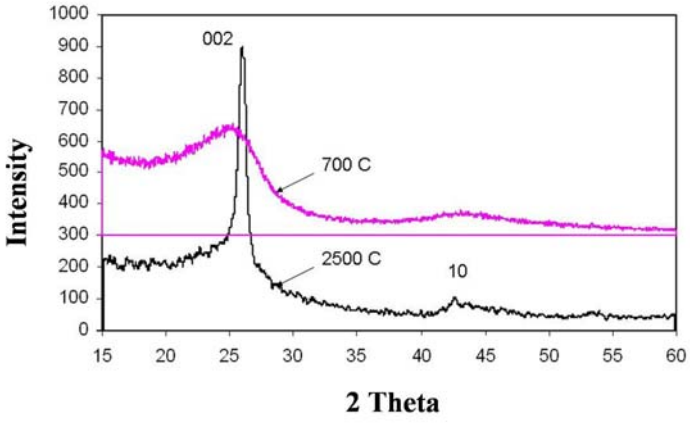

Figure 4. XRD patterns of mesoporous carbons (CPG-25-C) as a function of post-synthesis annealing temperature.

All the templates and resulting mesoporous carbons were subjected to standard nitrogen vapor adsorption/desorption characterization. Table 1 and Figure 5 show the result of the pore structure of templates and corresponding carbons, including BET (Brunauer, Emmett, and Teller) surface area, total pore volume, and pore size distribution (PSD). Figures 5 (a)-(f) present the pore size distributions of the carbons using BJH (Barrett, Joyner, and Halenda) method. The results show the strong influence of the templates (both uniform CPG and irregular silica gel templates) on the dominant pore size of the carbons, which ranges from several to 100 nanometers.

Table 1. Pore structure characterization* of templates and templated carbons

Template and nominal pore size	BET surface area of template (m^2/g)	Pore volume of template (cc/g)	Measured BET surface area of carbon (m^2/g)	Measured Pore volume of carbon (cc/g)	Predicted BET surface area of carbon (m^2/g)
CPG					
12 nm	116	0.61	247	0.77	182
25 nm	82	0.97	144	0.44	81
45 nm	47	0.77	62	0.40	59
70 nm	39	0.84	44	0.25	44
100 nm	31	1.3	25	0.23	23
Silica Gel					
6 nm	497	0.83	559	0.63	573
15 nm	269	1.15	316	0.44	225

* Based on full N_2 vapor adsorption isotherms at 77K.

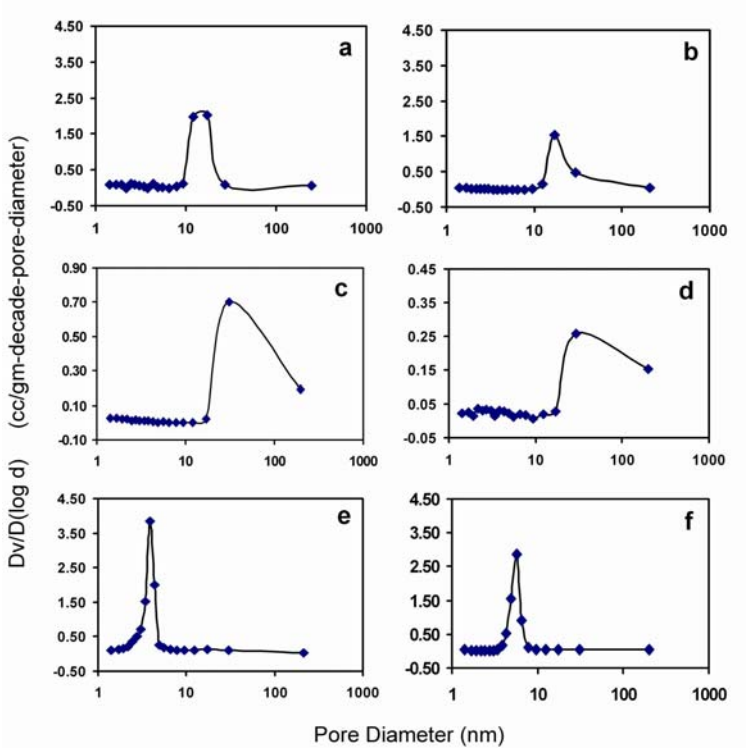

Figure 5. Pore size distribution of various mesoporous carbons derived from (a) 12 nm CPG, (b) 25 nm CPG, (c) 45 nm CPG, (d) 70 nm CPG, (e) 6 nm silica gel, and (f) 15 nm silica gel.

Figure 6 shows a strong correlation between the carbon surface area and the area of the original template. Careful consideration of the inverse replica concept, however, indicates that this should not be a complete and correct fundamental relationship. Other parameters, such as total pore volume of template and carbon yield (which together determine carbon mass) along with possible carbonization shrinkage together govern the mass-specific surface area of the resultant carbon. The next section proposes a more complete model that provides a better description of most of the data in Figure 6.

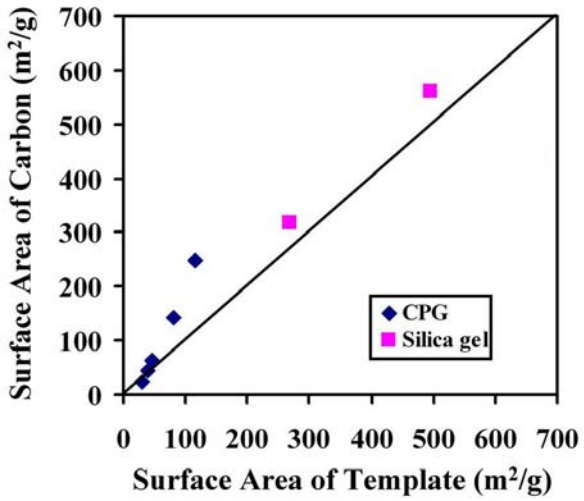

Figure 6. Total surface areas of the mesoporous carbons as a function of template areas.

Model development

Here we develop a quantitative model of the negative replica process assuming: (1) complete infiltration of all pores, (2) negligible development of intrinsic (non-templated) microporosity, (3) a carbonization yield approximately equal to the bulk (unconfined) value for AR, 85 wt-%, (4) negligible template shrinkage or structural collapse during carbonization or cooling. All the templates we used have pore size ranging from several nm to hundreds of nm. In this range, AR molecules (1-2 nm disk-like molecules) are able to infiltrate into most of these pores by capillary forces. Separate BET surface area experiment for carbonized AR mesophase (produced without using any template) shows almost zero surface area for the sample, indicating very limited intrinsic microporosity

development. In the absence of porosity development, the organic phase must, by unavoidable geometric constraints, shrink locally within the template by a factor of $(Y \cdot \rho_p/\rho_c)^{1/3}$, where Y is the carbon yield upon heating. In an unconstrained body, shrinkage reduces area, but within a fixed template the effect of local shrinkage depends on curvatures leading either to a decrease in area (convex surfaces as in a spherical solid grain), or an increase in area (concave surfaces, as in a spherical pore). The complex pore shapes in this study should exhibit both types of curvature, so we assume that area is approximately independent of local shrinkage, and based on the negative replica concept that the absorption surface area of the two phases (carbon/inorganic) is identical but their masses are different, leading to the following geometric relation for carbon area:

$$\left(\frac{A}{m}\right)_c = \frac{\left(\frac{A}{m}\right)_t}{V_{pores,t} \cdot \rho_p \cdot Y} \qquad (1)$$

where $(A/m)_c$ is the total carbon area per unit mass, $V_{pores,t}$ is the total pore volume of the template per unit mass, ρ_p = 1.23 gm/cm^3, which is the typical density of AR mesophase pitch, and Y= 85 wt-%, which is the bulk carbon yield for AR. The predicted values are shown in Figure 7. The measured surface area and predicted surface area, as shown in Figure 7, match well providing support for the quantitative negative replica concept.

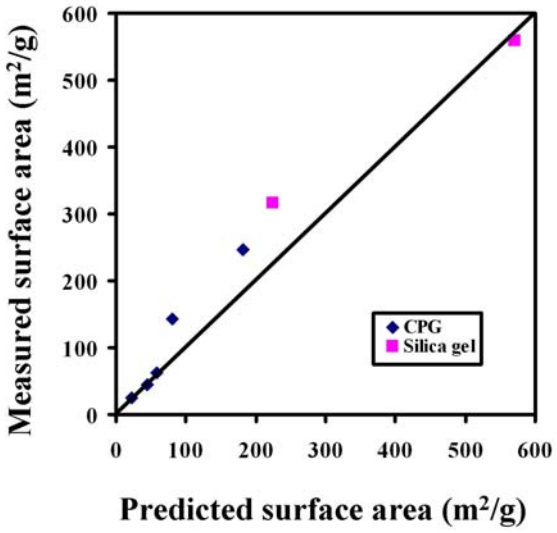

Figure 7. Comparison of model prediction to measured total surface areas for a range of mesoporous carbons.

3.2 Characterization of surface activity

Two complementary techniques were used to assess the activity of the edge-rich surfaces selected mesophase-derived carbons.

3.2.1 Total acid site determination following nitric acid treatment

Table 2 shows the base titration data of HNO_3-treated mesoporous carbons. The data show that acidic site density ranges from around 2.5 to 5.9 μmol/m^2, equivalent to 1.5 to 3.6 acid-sites/$(nm)^2$. In principle the calculated fractional coverage strictly depends on whether the underlying carbon edge is the zigzag or armchair plane. The theoretical edge site density on the zigzag and armchair surfaces of graphite is 12.0 and 13.8 carbon-edge-sites/$(nm)^2$ respectively. The functional groups on the carbon surface after HNO_3 treatment are believed to be complex, including a variety of groups such as carboxyl, phenolic hydroxyl, carbonyl, lactone and ester groups; nitro groups are also possible due to the nitration [39 Salame 2001]. It is difficult to determine all the functional groups quantitatively and qualitatively, and the NaOH base titration here is used to determine the total amount of acidic groups including carboxyl, hydroxyl and possibly lactone groups available on the surfaces [34 Pittman 1997].

Table 2. Base-titration data of HNO_3 treated mesoporous carbons.

Sample	Annealing temperature (°C)	HNO_3 (wt-%)	Density of acid sites (μmol/m^2)	Density of acid sites #/$(nm)^2$	Apparent acid site coverage Zigzag (%)	Apparent acid site coverage Armchair (%)
CPG-25-C						
1	700	10	2.78	1.67	14.0	12.1
2	700	70	3.52	2.12	17.7	15.4
3	1000	10	2.76	1.66	13.9	12.0
4	1000	70	3.10	1.87	15.6	13.5
CPG-70-C						
1	700	10	2.48	1.49	12.5	10.8
2	700	70	5.90	3.55	29.7	25.7
3	1000	10	4.02	2.42	20.2	17.5
4	1000	70	4.49	2.70	22.6	19.6

Note: Density of acid sites = Acidic sites / BET surface area.

Table 2 reveals several interesting trends. First, the acid site coverage for mesoporous carbons is higher for concentrated (70 wt-%) HNO_3 treatment than dilute (10 wt-%). Secondly, the acid site coverage is higher for mesoporous carbons with larger pore size. This effect may be due to the more uniform edge-on anchoring state seen in larger pore (larger carbon domain) materials. As domain size (and pore size) decrease, it becomes increasingly difficult for the discotic molecules to adopt strictly edge-on orientation at all surfaces as this requires director curvature over ever finer length scales. Finally, although higher temperature may cause carbon surface reconstruction in the form of loops or arches [16, 40, Jian 2006; Gogotsi 2002], changing the annealing temperatures from 700 ºC to 1000 ºC has little effect on the surface properties after HNO_3 treatment. The possible reason is that HNO_3 is a strong oxidant and it will open the reconstructed surface loops or arches, and thus makes the 1000 ºC carbons indistinguishable from 700 ºC carbons under HNO_3 treatment. It has been reported that HNO_3 can effectively remove the surface loops on carbon nanofibers [41 Lim S 2004].

It is valuable to compare the present data on surface activity with published results for other materials. Li et al. [42, Li 2005] report the acidic site density of activated carbons treated with a series of HNO_3 solutions (0.5-67 wt-%) at 93 ºC. The total acidic groups per BET area ranges from 0.21-3.7 μmol/m^2 (equivalently 0.37–3.69 mmol/g), of which about half of the acidic sites are carboxylic groups. The reported density of surface acidic groups on multi-walled carbon nanotubes (MWNTs) treated with nitric acid ranges from 0.2-0.5 a.t.% [43-44 Tsang 1994, Satishkumar 1996]. Hu et al. [45 Hu 2001] report the density of carboxylic functionality and total acidic functionality of 1-2% and 1-3% respectively for purified single-walled carbon nanotubes (SWNTs) treated under severe HNO_3/H_2SO_4 conditions. The much higher values here (2.48–5.9 μmol/m^2, 10-30% see Table 2) reflect higher surface defect densities due to the combination of low temperature synthesis and uniformly exposed edge sites due to the liquid crystal origin of these carbons. Overall there is evidence that the edge-rich surfaces on the mesophase-derived porous carbons in this study have a higher activity to nitric acid than activated carbons and multi-wall or single-wall nanotubes, both conventional carbon forms that do not possess ordered molecular architecture with all-edge surfaces.

3.2.2 Active surface area by oxygen chemisorption

Table 3 shows the calculated active surface area (ASA) and surface active site coverage (ASA/TSA); i.e. the portion of total surface area (TSA) that is active for chemisorption. In general the active sites include the edges of the basal plane, twin boundaries, imperfections such as vacancies, dislocations, and impurity sites, steps in the basal plane, etc. ASA is calculated as the product of carbon active site cross-sectional area (0.083 nm^2 [35]) and the total number of accessible active sites, which is derived from the amount of CO and CO_2. The calculated ASA/TSA of the mesoporous carbons is about 5 %. For comparison, Ehrburger et al. [46] report similar ASA/TSA ratios (3-6%) for phenolic carbon fibers, which are disordered materials. The more ordered carbon fibers from mesophase or PAN precursors have 4-5% ASA/TSA, but only after partial burnoff [46]. The ordered carbon, Graphon, is reported to have an initial ASA/TSA ratio of 0.29% that rises with partial gasification to an asymptotic maximum of 3.1% [Laine et al 35]). All of the materials show similar maximum ASA/TSA ratios, but the ordered, self-assembled carbons in this study exhibit that ratio without partial burnoff. The active site coverage is higher for mesoporous carbons with larger pore size, for example CPG-100-C, consistent with the trend using HNO_3.

Table 3. ASA analysis of mesoporous carbons by oxygen chemisorption

Sample	ASA (m^2/g)	CO/CO_2	ASA/TSA (%)
CPG-25-C			
Experiment 1	5.87	4.02	4.8
Experiment 2	5.41	3.78	3.8
Experiment 3	5.48	3.88	3.8
CPG-100-C			
Experiment 1	1.35	2.82	5.4
Experiment 2	1.30	2.78	5.2

An important fundamental question is why these surfaces, which consist solely of graphene edge sites, cannot be functionalized at densities approaching 100%. One explanation is the tendency of the graphene edge plane to undergo spontaneous reconstruction to reduce surface energy and cap exposed carbon active sites [16, 40 Jian2006, Gogotsi 2002]. Figure 8 shows typical surface reconstructions observed in

various edge-carbon surfaces from the Brown laboratories. These surface reconstruction features have been observed to form at temperatures as low as 600 ºC [16 Jian, 2006] and are quite common at higher annealing temperatures [16 Jian, 40 Gogotsi, 41 Mochida].

These reconstruction features are expected to limit functionalization density on edge planes and may also be responsible for the lower surface coverage determined by the oxygen chemisorption technique (~ 4-5% ASA/TSA) relative to the total acid site titration on HNO_3 treated surfaces (as high as 30%). The chemisorption technique involves vacuum thermal desorption of oxides leading to new active sites that may reconstruct at the high desorption temperatures required. The HNO_3 treatment on the other hand takes place at room temperature, and attack on reconstruction films, arches, or interstitial amorphous carbon atoms can lead to new active sites on the underlying (unreconstructed) edge plane that are immediately functionalized and thus stabilized with oxygen groups. The ASA adsorption/desorption cycle provides more opportunity for carbon surface healing than isothermal low-temperature treatment with a strong oxidizing acid. We should also note that the higher apparent functionalization densities with nitric acid may also be due to the formation of complex product films on inner surfaces that are stable to washing.

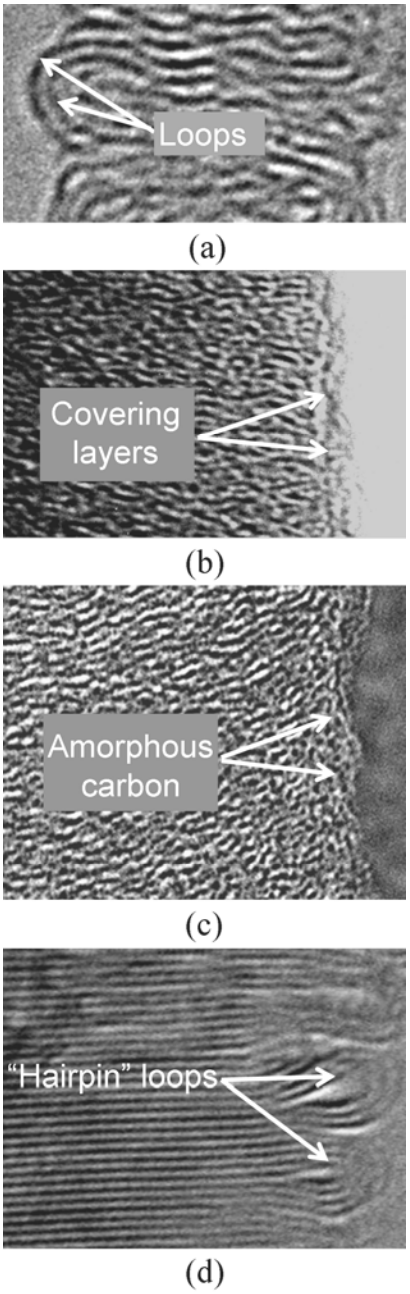

Figure 8. Typical reconstruction features observed on the outward facing graphene edge planes in mesophase-derived carbons : (a) closed half-circular loops or half-nanotube arches, 600 ºC carbon nanofibers [16 Jian 2006], (b) ultrathin films of 1-2 graphene layers covering active edges, 700 ºC carbon nanofibers [15 Jian 2003 Adv Mat], (c) amorphous materials, inner surfaces of mesoporous carbons [22 Yang, JNN], and (d) closed hairpin loops on 2500 ºC annealed carbon nanofibers [16 Jian 2006].

4. Conclusions

The use of liquid crystalline precursors for templated mesoporous carbons allows simultaneous control of both pore structure and interfacial crystal structure through the well-defined rules of liquid crystal surface anchoring. AR mesophase is a particularly advantageous precursor for the synthesis of "designer" mesoporous carbons. It exhibits a high carbon yield with almost no intrinsic porosity, so the pore structure can be completely controlled by template selection and can be approximately predicted by quantitative application of the geometric negative replica concept. When silica or other oxide templates are used the favored anchoring state is edge-on, yielding inner surfaces rich in active edge sites. There is evidence that these surfaces have higher chemical activity than conventional carbon surfaces and show total acid site densities as high as 30% following nitric acid treatment. Mesophase-derived templated porous carbons may find applications where a controlled mesopore size is required in combination with high surface activity or functional group density.

Acknowledgement

We acknowledge financial support from the NIEHS-supported SBRP grant at Brown University, P42 ES013660. We would like to thank Marietta Fernandez at Air Force Research Laboratory for the ASA measurements.

References

[1] Eltekova NA, Berek D, Novak I, Belliardo F. Adsorption of organic compounds on porous carbon sorbents. Carbon 2000; 38 (3): 373-377.

[2] Olkhovyk O, Jaroniec M. Ordered mesoporous silicas with 2,5-dimercapto-1,3,4-thiadiazole ligand: High capacity adsorbents for mercury ions. Journal of the International Adsorption Society 2005; 11 (3-4): 205-214.

[3] Abu-Daabes MA, Pinto NG. Synthesis and characterization of a nano-structured sorbent for the direct removal of mercury vapor from flue gases by chelation. Chemical Engineering Science 2005; 60 (7): 1901-1910.

[4] Sipos E, Fogassy G, Tungler A, Samant PV, Figueiredo JL. Enantioselective hydrogenations with highly mesoporous carbon supported Pd catalysts. Journal of molecular catalysis A-Chemical 2004; 212 (1-2): 245-250.

[5] Su FB, Zeng JH, Bao XY, Yu YS, Lee JY, Zhao XS. Preparation and characterization of highly ordered graphitic mesoporous carbon as a Pt catalyst support for direct methanol fuel cells**.** Chemistry of Materials 2005; 17 (15): 3960-3967.

[6] Samant PV, Rangel CM, Romero MH, Fernandes JB, Figueiredo JL. Carbon supports for methanol oxidation catalyst. Journal of Power Sources 2005; 151: 79-84.

[7] Moriguchi I, Nakahara F, Furukawa H, Yamada H, Kudo T. Colloidal crystal-templated porous carbon as a high performance electrical double-layer capacitor material. Electrochemical and Solid State Letters 2004; 7 (8): A221-A223.

[8] Yoon S, Lee JW, Hyeon T, Oh SM. Electric double-layer capacitor performance of a new mesoporous carbon. Journal of the Electrochemical Society 2000; 147 (7): 2507-2512.

[9] Lee J, Yoon S, Hyeon T, Oh SM, Kim KB. Synthesis of a new mesoporous carbon and its application to electrochemical double-layer capacitors. Chem. Comm. 1999; (21): 2177-2178.

[10] Han SJ, Yun YK, Park KW, Sung YE, Hyeon T. Simple solid-phase synthesis of hollow graphitic nanoparticles and their application to direct methanol fuel cell electrodes. Adv. Mat. 2003; 15 (22): 1922.

[11] Fan J, Wang T, Yu CZ, Tu B, Jiang ZY, Zhao DY. Ordered, nanostructured tin-based oxides/carbon composite as the negative-electrode material for lithium-ion batteries. Adv. Mat. 2004; 16 (16): 1432.

[12] Grigoriants I, Sominski L, Li HL, Ifargan I, Aurbach D, Gedanken A. The use of tin-decorated mesoporous carbon as an anode material for rechargeable lithium batteries. Chem. Comm. 2005; 7: 921-923.

[13] Hurt R, Krammer G, Crawford G, Jian KQ, Rulison C. Polyaromatic assembly mechanisms and structure selection in carbon materials. Chem Mater 2002; 14 (11): 4558-4565.

[14] Chan C, Crawford GP, Gao Y, Hurt RH, Jian KQ, Li H, et al. Liquid crystal engineering of nanofibers and nanotubes. Carbon 2005; 43 (12): 2431-2440.

[15] Jian KQ, Shim HS, Schwartzman A, Crawford GP, Hurt RH. Orthogonal carbon nanofibers by template-mediated assembly of discotic mesophase pitch. Adv Mater 2003; 15 (2): 164-167.

[16] Jian KQ, Yan A, Kulaots I, Crawford GP, Hurt RH, Reconstruction and hydrophobicity of nanocarbon surfaces composed solely of graphene edges, Carbon 2006; 44 (10): 2102-2106.

[17] Konno H, Sato S, Habazaki H, Inagaki M. Formation of platelet structure carbon nanofilaments by a template method. Carbon 2004; 42 (12-13): 2756-2759.

[18] Zhi LJ, Gorelik T, Wu JS, Kolb U, Mullen K. Nanotubes fabricated from Ni-naphthalocyanine by a template method. J Am Chem Soc 2005; 127 (37): 12792-12793.

[19] Zhi LJ, Wu JS, Li JX, Kolb U, Mullen K. Carbonization of disclike molecules in porous alumina membranes: Toward carbon nanotubes with controlled graphene-layer orientation. Angewandte Chemie-International Edition 2005; 44 (14): 2120-2123.

[20] Jian KQ, Xianyu HQ, Eakin J, Gao YM, Crawford GP, Hurt RH. Orientationally ordered and patterned discotic films and carbon films from liquid crystal precursors. Carbon 2005; 43(2): 407-415.

[21] Kim TW, Park IS, Ryoo R. A synthetic route to ordered mesoporous carbon materials with graphitic pore wall. Angewandte Chemie-International Edition 2003; 42 (36): 4375-4379.

[22] Yang N, Jian KQ, Kulaots I, Crawford GP, Hurt RH. Template synthesis of a porous nanophase mesocarbon. J Nanosci Nanotechnol 2003; 3 (5): 386-391.

[23] Gierszal KP, Jaroniec M, Novel pitch-based carbons with bimodal distribution of uniform mesopores, Chem Comm 2004; (22): 2576-2577.

[24] Gierszal KP, Kim TW, Ryoo R, Jaroniec M. Adsorption and structural properties of ordered mesoporous carbons synthesized by using various carbon precursors and ordered siliceous P6mm and Ia(3)over-bard mesostructures as templates. J Phys Chem B 2005; 109 (49): 23263-23268.

[25] Yoon SB, Chai GS, Kang SK, Yu JS, Gierszal KP, Jaroniec M. Graphitized pitch-based carbons with ordered nanopores synthesized by using colloidal crystals as templates. J Am Chem Soc 2005; 127 (12): 4188-4189.

[26] Jian KQ, Shim HS, Tuhus-Dubrow D, Bernstein S, Woodward C, Pfeffer M, Steingart D, Gournay T, Sachsmann S, Crawford GP, Hurt RH. Liquid crystal surface anchoring of mesophase pitch. Carbon 2003; 41 (11): 2073-2083.

[27] Brooks JD and Taylor GH, Carbon 1965; 3: 185.

[28] Hennig GR, in Chemistry and Physics of Carbon, Vol. 2 (Walker PL, Jr., ed.) Marcel Dekker, New York, 1966, P. 1.

[29] Thomas JM. in Chemistry and Physics of Carbon, Vol. 2 (Walker PL, Jr., ed.) Marcel Dekker, New York, 1965, P. 121.

[30] Phillips R, Vastola FJ, and Walker PL, Jr. Carbon 1970; 8: 197.

[31] Ye H, Naguib N, Gogotsi Y, Yazicioglu AG, Megaridis CM. Wall structure and surface chemistry of hydrothermal carbon nanofibres. Nanotechnology 2004; 15: 232-236.

[32] Boehm HP. Some aspects of the surface-chemistry of carbon-blacks and other carbons. Carbon 1994; 32 (5): 759-769.

[33] Boehm HP. Surface oxides on carbon and their analysis: a critical assessment. Carbon 2002; 40: 145–149.

[34] Pittman CU, He GR, Wu B, and Gardner SD. Chemical modification of carbon fiber surfaces by nitric acid oxidation followed by reaction with tetraethylenepentamine. Carbon 1997; 35 (3): 317-331.

[35] Laine NR, Vastola FJ, and Walker PL Jr. J. Phys. Chem. 1963; 67: 2030.

[36] Hoffman WP, Vastola FJ, and Walker PL Jr. Chemisorption of alkanes and alkenes on carbon active sites. Carbon 1984; 22: 585.

[37] Hoffman WP. The importance of active surface area in the heterogeneous reactions of carbon. Carbon 1991; 29: 769.

[38] Hoffman WP. “Chemisorption Processes on Carbon” in The Science of Carbon Materials, University of Alicanti Press 2000.

[39] Salame II and Bandosz1 TJ. Surface chemistry of activated carbons: combining of temperature-programmed desorption, and potentiometric titrations. Journal of Colloid and Interface Science 2001; 240: 252–258.

[40] Rotkin SV, Gogotsi Y. Analysis of non-planar graphitic structures: from arched edge planes of graphite crystals to nanotubes. Mat Res Innovat 2002; 5:191-200.

[41] Lim S, Yoon SH, Isao Mochida I, and Chi JH. Surface modification of carbon nanofiber with high degree of graphitization. J. Phys. Chem. B 2004; 108: 1533-1536.

[42] Li JY, Ma L, Li XN, Lu CS, and Liu HZ. Effect of nitric acid, pretreatment on the properties of activated carbon and supported palladium catalysts. Ind Eng Chem Res 2005; 44: 5478-5482.

[43] Tsang SC, Chen YK, Harris PJF, and Green MLH. Nature 1994; 372:159.

[44] Satishkumar BC, Govindaraj A, Mofokeng J, Subbanna GN and Raoy CNR. Novel experiments with carbon nanotubes: opening, filling, closing and functionalizing nanotubes. J. Phys. B: At. Mol. Opt. Phys. 1996; 29: 4925–4934.

[45] Hu H, Bhowmik P, Zhao B, Hamon MA, Itkis ME, Haddon RC. Determination of the acidic sites of purified single-walled carbon nanotubes by acid-base titration. Chemical Physics Letters 2001; 345(1,2): 25-28.

[46] P. Ehrburger, N. Pusset, P. Dziedzinl. Active surface area of microporous carbons. Carbon 1992; 30 (7): 1105-1109.